

Secondary organic aerosol yields from cloud-processing of isoprene oxidation products

Barbara Ervens,^{1,2} Annmarie G. Carlton,³ Barbara J. Turpin,⁴ Katy E. Altieri,⁵ Sonia M. Kreidenweis,¹ and Graham Feingold²

Received 27 August 2007; revised 1 October 2007; accepted 13 December 2007; published 31 January 2008.

[1] While there is a growing understanding from laboratory studies of aqueous phase chemical processes that lead to secondary organic aerosol (SOA) formation in cloud droplets (SOA_{drop}), the contribution of aqueous phase chemistry to atmospheric SOA burden is yet unknown. Using a parcel model including a multiphase chemical mechanism, we show that SOA_{drop} carbon yields (Y_c) from isoprene (I) depend strongly on the initial volatile organic carbon (VOC)/NO_x ratio resulting in $42\% > Y_c > 0.4\%$ over the atmospherically-relevant range of $0.25 < \text{VOC}/\text{NO}_x < 100$; (2) increase with increasing cloud-contact time; (3) are less affected by cloud liquid water content, pH, and droplet number. (4) The uncertainty associated with gas/particle-partitioning of semivolatile organics introduces a relative error of $-50\% \leq \Delta Y_c < +100\%$. The reported yields can be applied to air quality and climate models as is done with SOA formed on/in concentrated aerosol particles (SOA_{aer}).

Citation: Ervens, B., A. G. Carlton, B. J. Turpin, K. E. Altieri, S. M. Kreidenweis, and G. Feingold (2008), Secondary organic aerosol yields from cloud-processing of isoprene oxidation products, *Geophys. Res. Lett.*, 35, L02816, doi:10.1029/2007GL031828.

1. Introduction

[2] Uncertainties in estimating aerosol direct and indirect effects on climate arise due to the complexity of aerosol properties and their sources and sink processes. While these are usually well captured in models for inorganic aerosol constituents, the organic fraction represents a much greater challenge. Organic aerosols can be classified into primary (i.e., directly emitted) and secondary organic aerosol (SOA) where the latter refers to particle mass that is formed from precursor gases through coupled chemical and thermodynamic processes. Current aerosol models significantly underestimate SOA mass [*de Gouw et al.*, 2005; *Heald et al.*, 2005; *Volkamer et al.*, 2006].

[3] The apportionment of sources to total observed SOA is not well understood due to interactions of biogenic and anthropogenic gases. Isoprene is a potentially important

SOA precursor as its global emission rate exceeds those of all other non-methane-hydrocarbons and even a small yield might enhance predicted SOA mass considerably [*Lim et al.*, 2005; *Henze and Seinfeld*, 2006; *Lane and Pandis*, 2007]. Substantial research has been performed in smog chambers on SOA formation on/in aerosol particles (SOA_{aer}) through gas phase reactions followed by gas-to-particle conversion of products, i.e., through nucleation, condensation, and/or sorption, perhaps followed by aerosol phase reactions. Isoprene SOA_{aer} yields range from 1–3% with the highest values in NO_x-free experiments [*Kroll et al.*, 2005; *Ng et al.*, 2007].

[4] Clouds constitute a condensed phase volume that is larger by several orders of magnitude than that represented by haze particles, i.e. particles that are composed of solute and water (size range 0.1–1 μm) at a relative humidity (RH) < 100%; this larger volume enables increased uptake of water-soluble organics. In the aqueous phase, organics are oxidized into low-volatility products that remain in the particle upon drop evaporation. Modeling [*Ervens et al.*, 2004a; *Lim et al.*, 2005; *Chen et al.*, 2007], laboratory [*Altieri et al.*, 2006; *Carlton et al.*, 2007], and field [*Sorooshian et al.*, 2006] studies suggest that this sequence of processes represents an additional SOA source in the atmosphere (SOA_{drop}).

[5] We present results from cloud parcel model studies using a chemical multiphase mechanism that includes most recent laboratory data for aqueous phase reactions of water-soluble isoprene oxidation products [*Altieri et al.*, 2006; *Carlton et al.*, 2006, 2007]. Simulations were performed for a wide range of initial VOC (volatile organic carbon, here: isoprene)/NO_x ratios, chemical (pH), thermodynamic (partitioning of semivolatile organics), and cloud properties (cloud-contact time τ , average liquid water content LWC_{av} , aerosol number concentration N_o).

2. Model Description

2.1. Cloud Parcel Model

[6] The cloud parcel model has been described in prior studies [*Feingold and Heymsfield*, 1992; *Feingold et al.*, 1998; *Ervens et al.*, 2004a]. Briefly, the model considers the growth of a population of aerosol particles (lognormal size distribution with number concentration $N_o = 100 \text{ cm}^{-3}$, apportioned to ten logarithmically-spaced size classes 0.01 μm –1.2 μm) by water vapor uptake and their activation into cloud droplets in an adiabatic rising air parcel. 45 trajectories that describe passages of an air parcel through stratocumulus clouds, derived from three-dimensional Eulerian large-eddy-simulations, during the course of one hour are used as drivers for the parcels. These trajectories

¹Atmospheric Science Department, Colorado State University, Fort Collins, Colorado, USA.

²NOAA Earth System Research Laboratory, Boulder, Colorado, USA.

³Atmospheric Sciences Modeling Division, NOAA Air Resources Laboratory, Durham, North Carolina, USA.

⁴Department of Environmental Sciences, Rutgers University, New Brunswick, New Jersey, USA.

⁵Institute of Marine and Coastal Sciences, Rutgers University, New Brunswick, New Jersey, USA.

Table 1. Partitioning Ratios P for Semivolatile Organics if $LWC < 10^{-3} \text{ g m}^{-3}$

Species	P	Reference
Formic Acid	0.05	Baboukas et al. [2000]
Acetic Acid	0.17	Baboukas et al. [2000]
Glycolic Acid	0.75	Lim et al. [2005]
Glyoxylic Acid	0.75	Lim et al. [2005]
Oxalic Acid	0.90	Lim et al. [2005]
Pyruvic Acid	0.70	Lim et al. [2005]
Glycolaldehyde	0.36	Matsunaga et al. [2004]
Glyoxal	0.46	Matsunaga et al. [2004]
Hydroxyacetone	0.36	Matsunaga et al. [2004]
Methylglyoxal	0.36	Matsunaga et al. [2004]

reflect the characteristic dynamical and microphysical features of observed stratocumulus-topped layers [Stevens et al., 1996]. They cover ranges of $0.5 < \tau [\text{min h}^{-1}] < 51$, $0.002 < LWC_{av} [\text{g m}^{-3}] < 0.3$, $75\% \leq \text{RH}$, maximum in-cloud supersaturations of $0.8 < S_{\text{max}} [\%] < 1.4$ and one to three cloud passages per hour. The accumulation of SOA_{drop} mass from multiple cloud cycles is simulated by repeating each of the 1-h-trajectory five times (starting at 10:00 am). By repeating trajectories over five hours it is assumed that the cloud-capped boundary layer does not evolve over the 5-h-period. It is assumed that in-cloud mass formation does not modify the cloud-nucleating properties of the initial aerosol population in subsequent cloud cycles in contrast to previous studies that focused on cloud-processing effects on cloud microphysics [Feingold and Kreidenweis, 2000; Ervens et al., 2004b]. Chemical gas phase and uptake processes are simulated for the full simulation time; aqueous phase processes are considered if the total $LWC > 10^{-3} \text{ g m}^{-3}$ and the ionic strength $< 0.01 \text{ M}$ in an individual drop class. We do not simulate chemical processes in/on particles that exist in the absence of, or interstitially within clouds.

2.2. Chemical Mechanism and Initialization

[7] The gas phase mechanism represents a subset of the NCAR Master mechanism, Version 2.4 [Madronich and Calvert, 1990; Stroud et al., 2003] tailored to describe isoprene oxidation by ozone and OH. In the absence of clouds, we assume physical (i.e., non-reactive) partitioning that is prescribed by constant partitioning ratios P (= particulate/total mass) of semivolatile organics based on atmospheric measurements (Table 1). The particulate fractions predicted by P might include some material stripped from oligomers during chemical analysis as well as some error due to organic sampling artifacts. The value for glyoxal ($P = 0.46$) for $LWC \sim 10^{-4} \text{ g m}^{-3}$ (which corresponds to water masses associated with particles at the lowest RH recorded on the parcels) is in agreement with the ‘effective Henry’s law constant’ of glyoxal that has been determined in laboratory studies of concentrated aqueous particles ($K_{ij}^* = 2.2 \cdot 10^8 \text{ M atm}^{-1}$ [Volkamer et al., 2007]). The consistent results from laboratory and field data for P (glyoxal) give confidence that the ratios in Table 1 are reasonable approximations.

[8] Partitioning between the gas and droplet phases is described by mass accommodation coefficients, gas phase diffusion and Henry’s law constants [Ervens et al., 2004a]. The aqueous phase reaction scheme includes both sulfate and organic mass formation and is based on our previous

studies [Ervens et al., 2004a] with modifications of pyruvic acid and glyoxal oxidation, including the formation of large multifunctional compounds (LMC) from glyoxal (Figure 1) [Lim et al., 2005; Altieri et al., 2006; Carlton et al., 2006, 2007]. While it has been demonstrated that aqueous pyruvic acid and methylglyoxal oxidation also yield oligomers [Altieri et al., 2006, 2007], these are not included because their formation mechanism is not well enough understood. (The complete reaction scheme is available as auxiliary material, Tables S1, S2, S3, S4, and S5).¹

[9] Initial mixing ratios for SO_2 (0.2 ppb), O_3 (30 ppb), H_2O_2 (0.2 ppb), HNO_3 (0.2 ppb), and CO_2 (360 ppm) are used in all simulations assuming a closed system, i.e., without renewal of gases during a simulation. Two base cases, both representing relatively clean scenarios, are defined: (1) low VOC/ NO_x -ratio = 5 (isoprene = 1 ppb; $\text{NO}_x = 1$ ppb) and (2) high VOC/ NO_x -ratio = 100 (isoprene: 4 ppb, $\text{NO}_x = 0.2$ ppb).

2.3. Calculation of Yields (Y_c)

[10] SOA_{drop} yields (Y_c) are expressed as organic carbon (OC) mass since its concentration is the most commonly measured organic quantity in atmospheric particles. In section 3.7, we discuss how to convert OC to total organic matter (OM) mass. We report Y_c at the minimum liquid water content ($\sim 10^{-6} \text{ g m}^{-3}$, $\text{RH} \sim 75\%$) for each trajectory, i.e., after cloud evaporation, where

$$Y_c = \frac{SOA_{\text{mass}}[\text{ng C m}^{-3}]}{\text{Initial carbon mass}(\text{gas phase isoprene})[\text{ng C m}^{-3}]} \cdot 100\% \quad (1)$$

[11] We compare two sets of model simulations: (1) ‘Uptake only’ predicts Y_c from the partitioning of semivolatile organics (Table 1) that are formed by gas phase reactions and partition into particles (described by P) or are dissolved into droplets in the presence of clouds. These yields might not agree with SOA_{aer} in chamber experiments because our mechanism neither includes partitioning of organic peroxides (or other products not listed in Table 1) nor aerosol phase reactions. (2) The ‘multiphase scheme’ extends the ‘uptake only’ approach by chemical reactions in cloud droplets (Figure 1).

3. Results and Discussion

3.1. ‘Uptake-Only’ Simulations

[12] The yields Y_c using the ‘uptake only’ scheme exhibit small inter-trajectory variability with $Y_c = 3.1 \pm 0.2\%$ and $0.32 \pm 0.04\%$ for low and high VOC/ NO_x -ratios, respectively. The significant increase with increasing NO_x is due to the favored formation of water-soluble organics in VOC-limited scenarios [Ng et al., 2007]. The presence of clouds does not affect the gas phase source strengths of condensable species (Table 1) and, thus, in the following sections we only discuss results from the multiphase scheme.

3.2. LWC_{av} and τ

[13] The predicted yields for the multiphase scheme are higher (up to a factor of 3) than the ‘uptake only’ yields and

¹Auxiliary materials are available in the HTML. doi:10.1029/2007GL031828.

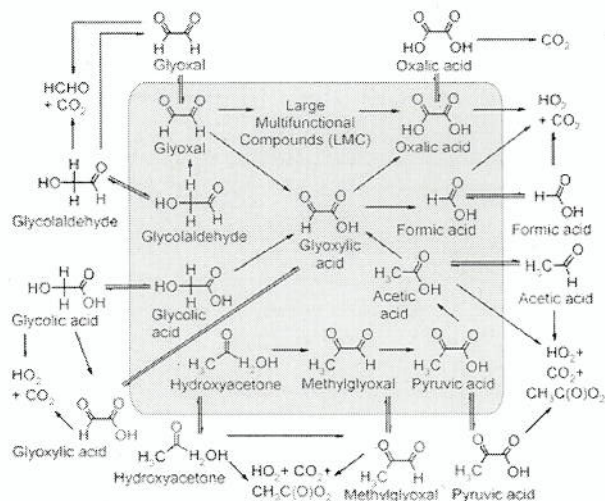


Figure 1. Chemical multiphase mechanism for the oxidation of isoprene oxidation products; double arrows, uptake processes; single arrows, OH-reactions [Ervens et al., 2004a; Lim et al., 2005; Altieri et al., 2006; Carlton et al., 2006, 2007]; shadowed area: aqueous phase.

vary depending on τ and LWC_{av} (Figure 2). Y_c and τ exhibit a significant positive correlation ($r^2 = 0.72$; $r^2 = 0.69$) whereas the correlation between Y_c and LWC_{av} is weaker ($r^2 \leq 0.55$; Figure S2). The aqueous phase is subsaturated with regards to organic reactants; thus, SOA formation is less sensitive to LWC_{av} than to τ . These trends differ from in-cloud sulfate formation [Feingold et al., 1998]: Whereas sulfate represents a chemical end-product and is formed at high reaction rates (from SO_2 oxidation by H_2O_2 or O_3) in a one-step process, organics are transformed at smaller rates in a multi-step sequence into low-volatility products and finally to CO_2 , outgassing of which leads to a decrease in SOA_{drop} mass.

[14] Our findings are consistent with a recent aircraft study that suggests a dependence of oxalate (not total SOA_{drop}) mass and oxalate/sulfate ratios on both the cloud volume fraction ($\propto \tau$) and maximum LWC [Sorooshian et al., 2007]. However, the latter study was performed using trajectories based on observed cloud depth and fractions ($\tau \leq 30 \text{ min h}^{-1}$) and characterized by higher LWC ($0.04 \text{ g m}^{-3} < LWC_{av} < 1 \text{ g m}^{-3}$).

3.3. VOC/NO_x Ratios

[15] As for ‘uptake only,’ multiphase simulations with a stepwise decrease in VOC/NO_x (increasing NO_x) show consistently increasing Y_c over an atmospherically-relevant range (VOC/NO_x = 50, 20, 10, 2, 1, and 0.25) with maximum values that are approaching a maximum limit (Table 2 and Figure S1). The dependence of Y_c on VOC/NO_x, τ [min h^{-1}] and LWC_{av} [g m^{-3}] (empirical) is given by:

$$Y_c = a_0 + a_1 \cdot \tau + a_2 \cdot LWC_{av} \quad (2)$$

with $a_0 = 0.30$, $a_1 = 0.004$, $a_2 = 397$, and $a_0 = 2.6$, $a_1 = 0.07$, $a_2 = 3821$ for high and low VOC/NO_x, respectively. The

parameters a_0 , a_1 , and a_2 show a consistent trend with varying VOC/NO_x-ratios (Table S6 and Figure S3). Model sensitivity analyses suggest that VOC/NO_x is a good predictor of Y_c for a range of absolute atmospheric VOC and NO_x concentrations: At fixed VOC/NO_x, Y_c does not change by more than $\sim 10\%$ compared to the base case (Table 2).

3.4. pH

[16] The pH is calculated in each drop class using the electroneutrality condition. This iterative procedure represents a significant numerical burden and a simplified treatment is desirable. In the base case simulations, the pH spans a range of $\sim 2 < \text{pH} < \sim 6$ throughout the drop spectrum. Comparison of Y_c assuming a constant pH of 2 or 6, respectively, for all droplets, shows that pH affects Y_c significantly only at long τ and low VOC/NO_x (Table 2). The weak dependence of Y_c on pH can be explained by the simultaneous increase in the rate constants of SOA_{drop} formation and loss reactions with pH [Ervens et al., 2003] leading to similar steady-state SOA_{drop} over a wide range of pH. In a recent laboratory study in moderately acidic solution ($4.2 < \text{pH} < 4.5$) oligomeric structures from methylglyoxal have been identified that are similar to those in concentrated (acidic) particles [Altieri et al., 2007] but the general pH dependence of oligomer formation in dilute solution is not well understood.

3.5. Initial Particle Concentration (N_a)

[17] Many aerosol/cloud models treat sulfate formation in bulk cloud water (all drops combined), and the newly-formed mass is distributed among the size classes after each model time-step. To examine whether this simplified approach can be used in the modeling of SOA_{drop} , we varied the initial aerosol number concentration (from $N_a = 100 \text{ cm}^{-3}$ to 5000 cm^{-3}), and, thus, the resulting drop number concentration ($\propto N_a$) while LWC_{av} remains the same along each trajectory. Again, the results show that the cases with the longest τ and lowest VOC/NO_x are most sensitive to the variation in input data (Table 2). For most conditions, however, SOA_{drop} formation is not limited by

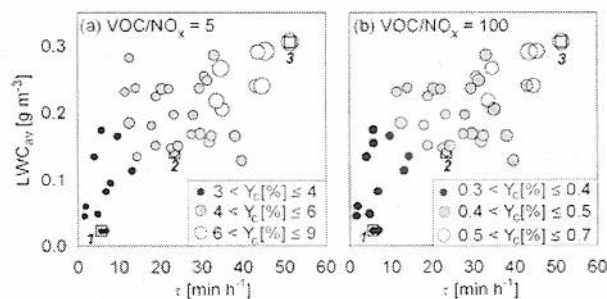


Figure 2. Maximum SOA yields (Y_c [%] ‘multiphase scheme’) as a function of cloud contact time τ and average liquid water content LWC_{av} for 45 trajectories using the multiphase scheme. The size of the circles depicts the variability of Y_c . (a) VOC/NO_x = 5; (b) VOC/NO_x = 100. (‘Uptake only’ Y_c : 3.1% and 0.32% for low and high VOC/NO_x, respectively.) The numbers 1, 2, 3 refer to the selected trajectories in Table 2 and are used in order to evaluate sensitivities of Y_c to other parameters.

Table 2. SOA_{drop} Yields Y_c (Trajectories 1, 2, 3) for All Multiphase Scheme Simulations

Isoprene, ppb	NO_x , ppb	VOC^a / NO_x	pH	P	N_{av} , cm^{-3}	Y_c , %		
						1	2	3
1	1	5		Table 1	100	4	5	9
0.5	0.5	5		Table 1	100	5	6	10
1	1	5	2	Table 1	100	4	5	6
1	1	5	6	Table 1	100	5	9	16
1	1	5		$0.5 \cdot P$	100	2	3	5
1	1	5		$2 \cdot P$ or $P = 1^b$	100	5	8	15
1	1	5		Table 1	5000	4	5	9
4	0.2	100		Table 1	100	0.4	0.5	0.7
2	0.1	100		Table 1	100	0.5	0.5	0.6
4	0.2	100	2	Table 1	100	0.4	0.5	0.5
4	0.2	100	6	Table 1	100	0.5	0.5	0.6
4	0.2	100		$0.5 \cdot P$	100	0.3	0.4	0.4
4	0.2	100		$2 \cdot P$ or $P = 1^b$	100	0.8	0.6	1.1
4	0.2	100		Table 1	5000	0.4	0.5	0.4
5	100	0.25		Table 1	100	19	28	42
0.4	2	1		Table 1	100	18	23	40
0.8	2	2		Table 1	100	10	13	22
1	0.5	10		Table 1	100	3	3	7
0.8	0.2	20		Table 1	100	2	3	4
2	0.2	50		Table 1	100	0.7	0.8	1

^aVOC is expressed in terms of carbon (isoprene: C_5).

^bFor oxalic, pyruvic, glyoxylic, and glycolic acid: $P = 1$, for all other compounds ($2 \cdot P$) (Table 1).

the air/drop-interface. This finding, together with the weak dependence on pH, suggests that SOA_{drop} can be modeled in bulk cloud water, similar to sulfate, avoiding the solution of differential equations for individual drop classes.

3.6. Partitioning Coefficients (P)

[18] Sensitivity runs using $P = 0.5 \cdot P$ and $2 \cdot P$ (constraining $P \leq 1$) reveal that a reduced P translates into slightly smaller Y_c whereas an increased P might enhance Y_c considerably. If the experimental values in Table 1 represent overestimates due to sampling artifacts (e.g., adsorption of gases on sampling media [Turpin et al., 2000]), our reported Y_c are slightly overestimated.

3.7. Organic Mass Speciation

[19] Based on the product distribution predicted from our reaction scheme, the relative mass fractions (related to total SOA_{drop} mass [$ng\ m^{-3}$] of all organics in Table 1), together with OM/OC ratios, have been calculated (Figure S4). The OM/OC ratios for the 'uptake-only' simulations are ~ 2.3 whereas they are higher for the 'multiphase scheme' (~ 2.8). We assumed OM/OC = 2 for LMC based on recent laboratory studies that suggest smaller OM/OC than for monomeric compounds [Altieri et al., 2007]. We predict in-cloud formation of glycolic, glyoxylic and oxalic acids, in agreement with aircraft measurements of cloud-processed particles where these acids accounted for several tens of $ng\ m^{-3}$ [Sorooshian et al., 2006, 2007]. LMC contribute up to 10% of the predicted SOA_{drop} mass. Their fractional contributions decrease with increasing LWC_{av} and τ since they represent intermediates that are quickly converted into oxalic acid (Figure 1). The large contribution of aldehydes ($\leq 80\%$) to SOA_{drop} seems surprising. However, recall that (1) SOA_{drop} is reported for wet particles at RH $\sim 75\%$ and (2) P likely also partially accounts for oligomers. Thus, the contribution of LMC might be even higher than suggested

in Figure S4 as we only define them according to the processes in Figure 1.

4. Summary and Conclusions

[20] Organic chemical aqueous phase processes represent an additional SOA source (SOA_{drop}). Under high NO_x conditions, water-soluble carbonyl compounds from isoprene oxidation are preferentially formed, taken up into cloud droplets, and further oxidized into low-volatility organics that remain in atmospheric particles upon cloud evaporation. Under low NO_x conditions (high VOC/NO_x), low-volatility organic peroxides are formed and readily condense onto particles (SOA_{aer}).

[21] Using a chemical multiphase scheme, we predict consistent trends of SOA_{drop} carbon yields Y_c from 0.4 to 42% over a range of $100 > VOC/NO_x > 0.25$ and for a wide range of additional parameters (Table 2). Sensitivity tests of LWC_{av} , cloud contact-time τ , aerosol (\propto droplet) number concentration, pH, and gas/particle-partitioning of semivolatile organics (P) show that the NO_x levels are most influential controlling Y_c , followed by τ . Enhanced SOA formation from isoprene in the presence of NO_x might help explain findings from field studies that show that particulate OC is mostly of biogenic origin but it correlates with anthropogenic tracers [de Gouw et al., 2005; Weber et al., 2007]. Thus, in regions with high NO_x and isoprene emissions, together with abundant clouds (e.g., Northeastern US or Southeast Asia) SOA_{drop} might significantly contribute to SOA.

[22] **Acknowledgments.** BE, GF, and SMK acknowledge funding from the NOAA Climate Goal. BT, AC, KA acknowledge funding from U.S. EPA Science to Achieve Results (STAR) program (R831073), the National Science Foundation (NSF-ATM-0630298), and the contributions of Dr. Sybil Seitzinger. AC acknowledges the Memorandum of Understanding between the United States Environmental Protection Agency through its Office of Research and Development and NOAA (agreement number DW13921548). This work constitutes a contribution to the NOAA Air Quality Program. Although the research described in this paper has been funded, subjected to review and approved for publication by the U.S. EPA, it does not necessarily reflect the views of the EPA; no official endorsement should be inferred. Any opinions, findings, and conclusions or recommendations expressed in this material are those of the authors and do not necessarily reflect the views of the National Science Foundation.

References

- Altieri, K., A. G. Carlton, H. Lim, B. J. Turpin, and S. P. Seitzinger (2006), Evidence for oligomer formation in clouds: Reaction of isoprene oxidation products, *Environ. Sci. Technol.*, **40**, 4956–4960.
- Altieri, K. E., S. P. Seitzinger, A. G. Carlton, B. J. Turpin, G. C. Klein, and A. G. Marshall (2007), Oligomers formed through in-cloud methylglyoxal reactions: Chemical composition, properties, and mechanisms investigated by ultra-high resolution FT-ICR mass spectrometry, *Atmos. Environ.*, in press.
- Baboukas, E. D., M. Kanakidou, and N. Mihalopoulos (2000), Carboxylic acids in gas and particulate phase above the Atlantic Ocean, *J. Geophys. Res.*, **105**, 14,459–14,471.
- Carlton, A. G., B. J. Turpin, H.-J. Lim, K. E. Altieri, and S. Seitzinger (2006), Link between isoprene and secondary organic aerosol (SOA): Pyruvic acid oxidation yields low volatility organic acid in clouds, *Geophys. Res. Lett.*, **33**, L06822, doi:10.1029/2005GL025374.
- Carlton, A. G., B. J. Turpin, K. E. Altieri, A. Reff, S. Seitzinger, H. Lim, and B. Ervens (2007), Oxalic acid and SOA production from glyoxal: Results of aqueous phase photooxidation experiments, *Atmos. Environ.*, **41**, 7588–7602.
- Chen, J., R. J. Griffin, A. Grini, and P. Tulet (2007), Modeling secondary organic aerosol formation through cloud processing of organic compounds, *Atmos. Chem. Phys.*, **7**, 5343–5355.
- de Gouw, J. A., et al. (2005), Budget of organic carbon in a polluted atmosphere: Results from the New England Air Quality Study in 2002, *J. Geophys. Res.*, **110**, D16305, doi:10.1029/2004JD005623.

- Ervens, B., S. Gligorovski, and H. Herrmann (2003). Temperature dependent rate constants for hydroxyl radical reactions with organic compounds in aqueous solution, *Phys. Chem. Chem. Phys.*, **5**, 1811–1824.
- Ervens, B., G. Feingold, G. J. Frost, and S. M. Kreidenweis (2004a). A modeling study of aqueous production of dicarboxylic acids: 1. Chemical pathways and speciated organic mass production. *J. Geophys. Res.*, **109**, D15205, doi:10.1029/2003JD004387.
- Ervens, B., G. Feingold, S. L. Clegg, and S. M. Kreidenweis (2004b). A modeling study of aqueous production of dicarboxylic acids: 2. Implications for cloud microphysics. *J. Geophys. Res.*, **109**, D15206, doi:10.1029/2004JD004575.
- Feingold, G., and A. J. Heymsfield (1992). Parameterizations of condensational growth of droplets for use in general circulation models, *J. Atmos. Sci.*, **49**, 2325–2342.
- Feingold, G., and S. Kreidenweis (2000). Does cloud processing of aerosol enhance droplet concentrations?, *J. Geophys. Res.*, **105**, 24,351–24,361.
- Feingold, G., S. M. Kreidenweis, and Y. Zhang (1998). Stratocumulus processing of gases and cloud condensation nuclei: 1. Trajectory ensemble model, *J. Geophys. Res.*, **103**, 19,527–19,542.
- Heald, C. L., D. J. Jacob, R. J. Park, L. M. Russell, B. J. Huebert, J. H. Seinfeld, H. Liao, and R. J. Weber (2005). A large organic aerosol source in the free troposphere missing from current models. *Geophys. Res. Lett.*, **32**, L18809, doi:10.1029/2005GL023831.
- Henze, D. K., and J. H. Seinfeld (2006). Global secondary organic aerosol from isoprene oxidation, *Geophys. Res. Lett.*, **33**, L09812, doi:10.1029/2006GL025976.
- Kroll, J. H., N. L. Ng, S. M. Murphy, R. C. Flagan, and J. H. Seinfeld (2005). Secondary organic aerosol formation from isoprene photooxidation under high-NO_x conditions, *Geophys. Res. Lett.*, **32**, L18808, doi:10.1029/2005GL023637.
- Lane, T. E., and S. N. Pandis (2007). Predicted secondary organic aerosol concentrations from the oxidation of isoprene in the Eastern United States, *Environ. Sci. Technol.*, **41**, 3984–3990.
- Lim, H., A. G. Carlton, and B. J. Turpin (2005). Isoprene forms secondary organic aerosol in Atlanta: Results from time-resolved measurements during the Atlanta supersite experiment, *Environ. Sci. Technol.*, **39**, 4441–4446.
- Madronich, S., and J. G. Calvert (1990). Permutation reactions of organic peroxy radicals in the troposphere, *J. Geophys. Res.*, **95**, 5697–5715.
- Matsunaga, S., M. Mochida, and K. Kawamura (2004). Variation of the atmospheric concentrations of biogenic carbonyl compounds and their removal processes in the northern forest at Moshiri, Hokkaido Island in Japan, *J. Geophys. Res.*, **109**, D04302, doi:10.1029/2003JD004100.
- Ng, N. L., et al. (2007). Effect of NO_x level on secondary organic aerosol (SOA) formation from the photooxidation of terpenes, *Atmos. Chem. Phys.*, **7**, 5159–5174.
- Sorooshian, A., et al. (2006). Oxalic acid in clear and cloudy atmospheres: Analysis of data from International Consortium for Atmospheric Research on Transport and Transformation 2004, *J. Geophys. Res.*, **111**, D23S45, doi:10.1029/2005JD006880.
- Sorooshian, A., M.-L. Lu, F. J. Brechtel, H. Jonsson, G. Feingold, R. C. Flagan, and J. H. Seinfeld (2007). On the source of organic acid aerosol layers above clouds, *Environ. Sci. Technol.*, **41**, 4647–4654.
- Stevens, B., G. Feingold, W. R. Cotton, and R. L. Walko (1996). Elements of the microphysical structure of numerically simulated nonprecipitating stratocumulus, *J. Atmos. Sci.*, **53**, 980–1006.
- Stroud, C., et al. (2003). Photochemistry in the Arctic free troposphere: NO_x budget and the role of odd nitrogen reservoir recycling, *Atmos. Environ.*, **37**, 3351–3364.
- Turpin, B. J., P. Saxena, and E. Andrews (2000). Measuring and simulating particulate organics in the atmosphere: Problems and prospects, *Atmos. Environ.*, **34**, 2983–3013.
- Volkamer, R., J. L. Jimenez, F. San Martini, K. Dzepina, Q. Zhang, D. Salcedo, L. T. Molina, D. R. Worsnop, and M. J. Molina (2006). Secondary organic aerosol formation from anthropogenic air pollution: Rapid and higher than expected, *Geophys. Res. Lett.*, **33**, L17811, doi:10.1029/2006GL026899.
- Volkamer, R., P. J. Ziemann, and M. J. Molina (2007). Secondary organic aerosol formation from acetylene: Seed, acid and RH dependence of glyoxal uptake to aerosols, *Rep. 4.2007*, ACCENT, Urbino, Italy.
- Weber, R. J., et al. (2007). A study of secondary organic aerosol formation in the anthropogenic-influenced southeastern United States, *J. Geophys. Res.*, **112**, D13302, doi:10.1029/2007JD008408.
- K. E. Altieri, Institute of Marine and Coastal Sciences, Rutgers University, 71 Dudley Road, New Brunswick, NJ 08901, USA.
- A. G. Carlton, Atmospheric Sciences Modeling Division, NOAA Air Resources Laboratory, Research Triangle Park, 109 T. W. Alexander Drive, Durham, NC 27711, USA.
- B. Ervens and S. M. Kreidenweis, Atmospheric Science Department, Colorado State University, Fort Collins, CO 80523, USA. (barbara.ervens@noaa.gov)
- G. Feingold, NOAA Earth System Research Laboratory, 325 Broadway, Boulder, CO 80305, USA.
- B. J. Turpin, Department of Environmental Sciences, Rutgers University, 14 College Farm Road, New Brunswick, NJ 08901, USA.